

# Quantifying the extremity of windstorms for regions featuring infrequent events

Michael A. Walz,<sup>1,2\*</sup> Tim Kruschke,<sup>2,3</sup> Henning W. Rust,<sup>2</sup> Uwe Ulbrich<sup>2</sup> and Gregor C. Leckebusch<sup>1</sup>

<sup>1</sup>School of Geography, Earth and Environmental Science, University of Birmingham, UK

<sup>2</sup>Institut fuer Meteorologie, Freie Universität Berlin, Germany

<sup>3</sup>Department of Ocean Circulation and Climate Dynamics, Research Unit Marine Meteorology, GEOMAR Helmholtz Centre for Ocean Research Kiel, Germany

\*Correspondence to:

M. A. Walz, School of Geography,  
 Earth and Environmental  
 Science, University of  
 Birmingham, Birmingham B15  
 2TT, UK  
 E-mail: maw526@bham.ac.uk

## Abstract

This paper introduces the Distribution-Independent Storm Severity Index (DI-SSI). The DI-SSI represents an approach to quantify the severity of exceptional surface wind speeds of large scale windstorms that is complementary to the SSI introduced by Leckebusch *et al.* While the SSI approaches the extremeness of a storm from a meteorological and potential loss (impact) perspective, the DI-SSI defines the severity in a more climatological perspective. The idea is to assign equal index values to wind speeds of the same singularity (e.g. the 99th percentile) under consideration of the shape of the tail of the local wind speed climatology. Especially in regions at the edge of the classical storm track, the DI-SSI shows more equitable severity estimates, e.g. for the extra-tropical cyclone Klaus. In order to compare the indices, their relation with the North Atlantic Oscillation is studied, which is one of the main large scale drivers for the intensity of European windstorms.

**Keywords:** windstorms; quantification of extremity; North Atlantic Oscillation; extra-tropical cyclones; generalized Pareto distribution

Received: 9 December 2016  
 Revised: 24 May 2017  
 Accepted: 25 May 2017

## 1. Introduction and motivation

### 1.1. Background

Winter windstorms are among the biggest natural hazards occurring in the mid-latitudes causing human casualties as well as economic losses up to billions of Euros each year. According to SwissRe, the winter storm Kyrill, which strongly affected Central Europe on 18, 19 January 2007 caused an economic insured loss of about \$6.1 billion and casualties of 54 people (SwissRe, 2016). An approach to objectively quantify the meteorological hazard is represented by the Storm Severity Index (SSI) introduced by Leckebusch *et al.* (2008). The SSI is widely used (e.g. Osinski *et al.*, 2016) for assessing the severity of windstorms within the actuarial sector by linking extreme surface winds (i.e. exceedances of the 98th percentile of local 6-hourly wind speeds) to potential loss on buildings. Furthermore, the 98th percentile is used as a criterion for identifying extreme windstorms in a wind tracking algorithm by Leckebusch *et al.* (2008) and further developed by Kruschke (2015). Equation (1) shows the mathematical definition of the SSI. The index  $t$  represents the time step,  $k$  represents the grid cell and  $A_k$  represents the area of the associated cell divided by a reference cell at the equator:

$$SSI_{T,K} = \sum_{t=1}^T \sum_{k=1}^K \left[ \left( \max \left( 0, \frac{v_{k,t} - v_{98,k}}{v_{98,k}} \right) \right)^3 \cdot A_k \right] \quad (1)$$

The  $v_{98,k}$  refers to the local 98th percentile of the  $k$ th grid cell which is the minimum wind speed at which damage on housing or nature is to be expected. This relationship was established based on real damage experience (Klawns and Ulbrich, 2003) which proved the assumption of Palutikof and Skellern (1991) who assumed storm damages to occur at about 2% of all days.

For the further development of the index, the focus will be on the Meteorological Contribution  $\Gamma$  to the SSI defined by Equation (2) which shifts and scales wind speeds by the 98th percentile:

$$\Gamma = \frac{v_{k,t} - v_{98,k}}{v_{98,k}} \quad (2)$$

### 1.2. Motivation for a supplementary severity index (DI-SSI)

Technically, the SSI is based on excesses over a fixed quantile (percentile) for a given wind speed distribution; however, the SSI does not take into account the shape of the distribution of these excesses, i.e. the tail behaviour. This property becomes particularly obvious in areas with little storm occurrence. The top panel of Figure 1 illustrates this effect: The two panels depict histograms of  $\Gamma$  (scaled and shifted wind speeds, cf. Equation (2)) of a grid cell south of Iceland (called Iceland hereafter) and on the Isle of Corsica. The coloured lines mark the 98th (red) and the 99th (green) percentile of the shifted and scaled distribution. As known from various

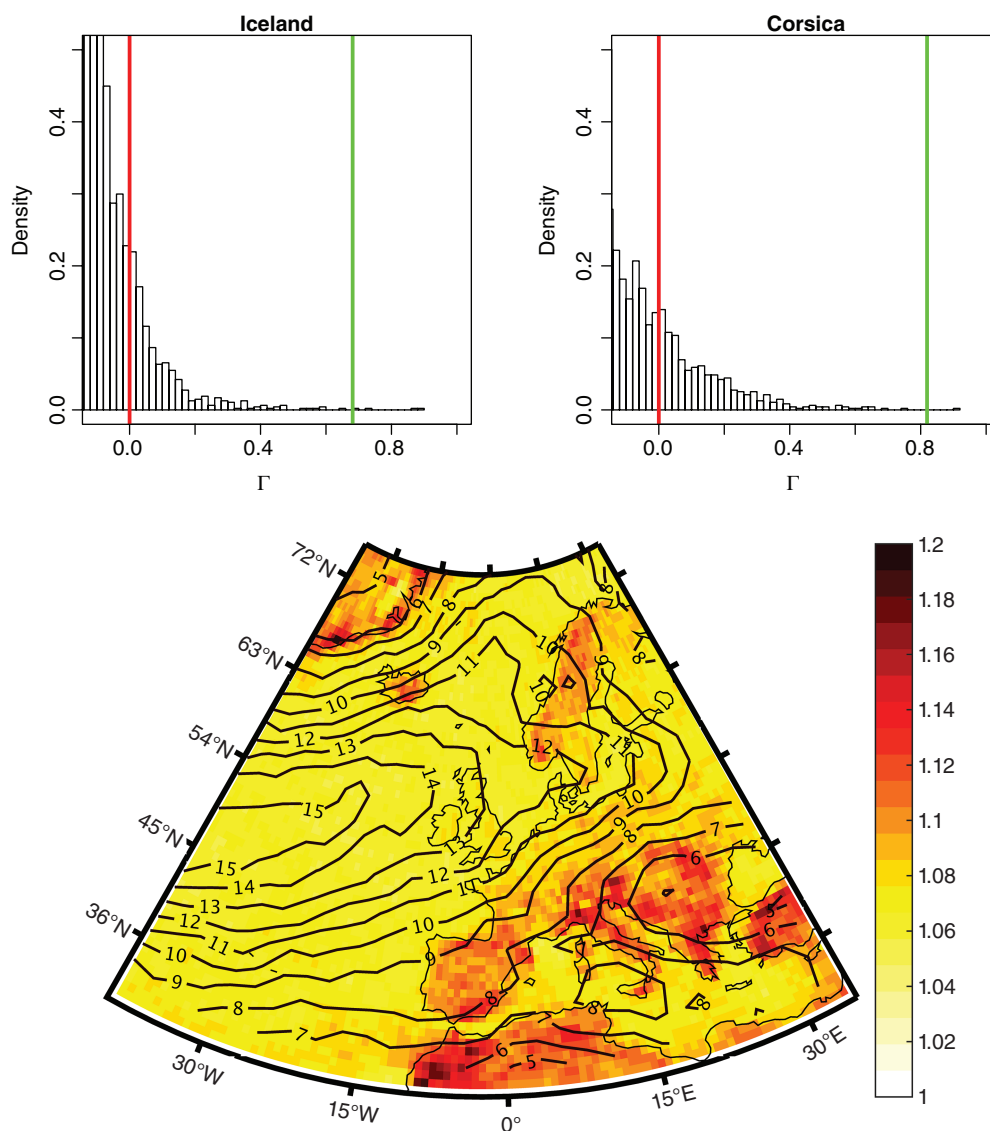


**Figure 1.** Top: Histograms of the Meteorological contribution ( $\Gamma$ ) as defined in Equation (2) for Iceland (left) and Corsica (right). The distribution of the events looks visibly different. The red line marks the 98th percentile, thus the cut off threshold. The green line marks the 99th percentile, thus it illuminates the larger difference between the two percentiles for Corsica in comparison with Iceland. Bottom: Quotient between the 99th and the 98th percentile of local wind speeds for Europe in colour. Large values indicate a large difference between the percentiles. The contours depict the average trackdensity per winter (ONDJFM; average number of tracks within a 500 km radius around a given grid point). The quotient is clearly larger in areas with a reduced windstorm frequency.

other studies (e.g. Leckebusch *et al.*, 2008 or Klawe and Ulbrich, 2003) the area south of Iceland is located within the corridor of extra-tropical cyclones (ETCs), whereas Corsica is less affected by ETCs (cf. bottom panel of Figure 1).

By definition of the SSI, the red line is equal to 0. The histogram for Iceland resembles a light-tailed distribution, whereas the histogram for Corsica shows features of a heavy-tailed distribution. Accordingly, the gap between the 99th and 98th percentile is substantially different (0.68 for Iceland and 0.82 for Corsica). Note that due to the cubic relationship of the SSI (Equation (1)),  $\Gamma$  is taken to the third power; for Corsica this is around six times larger than  $\Gamma^3$  for Iceland (cf. Table 1). From a probabilistic perspective, however, both wind speeds are equally likely. As the

SSI consists of spatially and temporally accumulated  $\Gamma^3$ , this implies that a potential storm over Corsica with wind speeds exceeding the 98th percentile will result in a much larger integral SSI value than a storm over Iceland with the same exceptional wind speeds (c.f. examples for storms Klaus and Martin in Table 2). The gap in  $\Gamma^3$  is a direct result of the local wind speed climatology and this in turn is a consequence of the scarcity of very extreme winds at the edge of the main storm track. Thus, within the storm track there are larger ‘background’ winds with a higher number of extreme events, whereas the edges of the storm track feature lower ‘background’ winds and comparatively few extreme events. The exceedance compared with the background wind in relative terms is larger for the edge of the storm track.

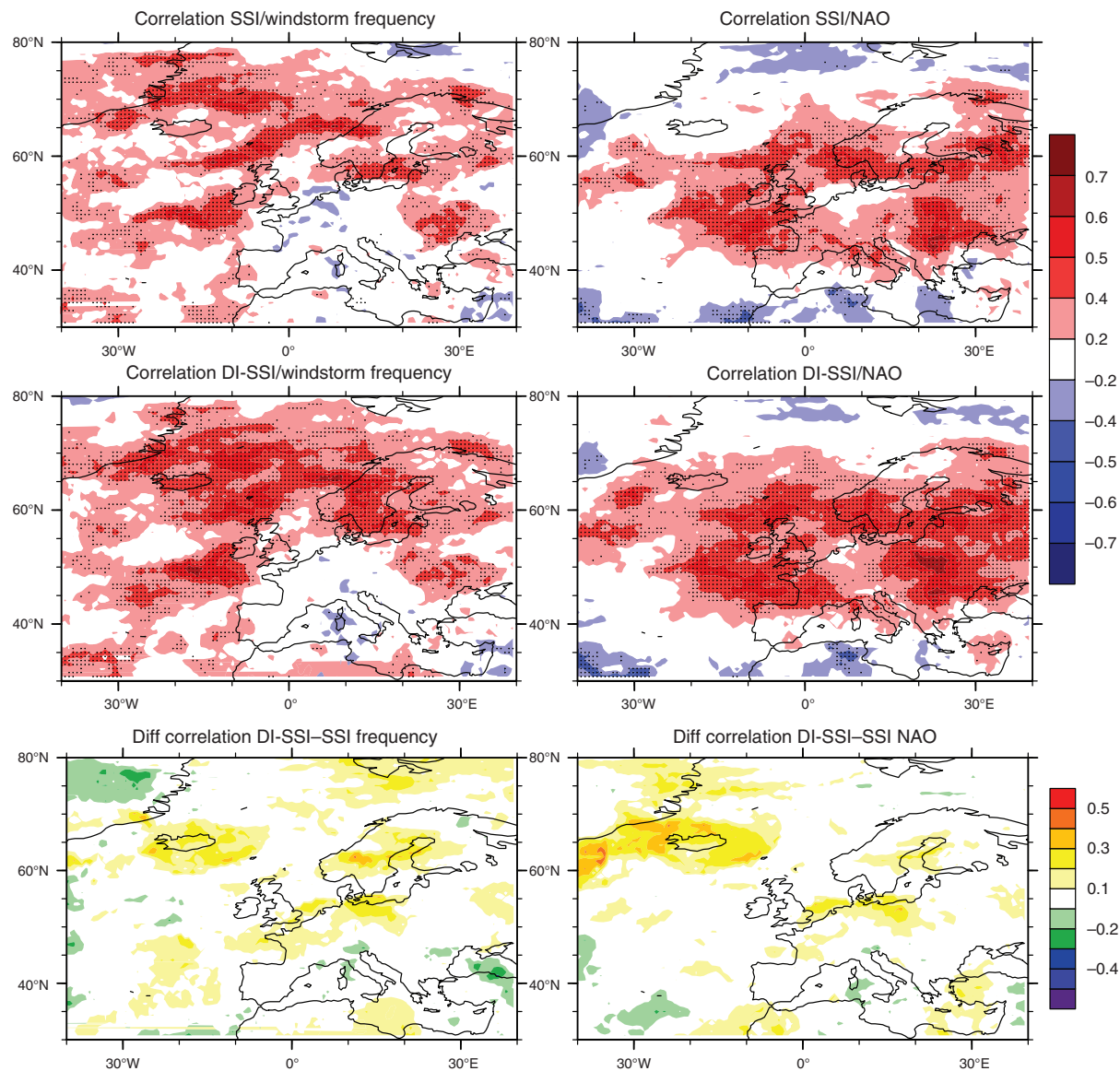


**Figure 2.** Left panel: Correlation between the storm frequency and storm intensity (SSI on the top; DI-SSI in the middle) for each grid cell. Correlation coefficients significant at the 5% level are stippled. There is a significant link between more storms and more intense storms for much of the North Atlantic and Scandinavia. Right panel: Correlation coefficients between the yearly NAO time series and the yearly windstorm intensity on grid cell level (SSI on the top; DI-SSI in the middle). Again correlation coefficients significant at the 5% level are tagged. Bottom row: Differences between the respective correlations. Positive values represent areas where the correlation for the DI-SSI is larger compared to the SSI. This is the case for most of the North Atlantic Domain.

**Table 1.** Meteorological and DI-SSI contributions of the two example grid cells. Note that the contribution of the grid cell in Corsica is more than five times larger, although the wind is of the same singularity in both cases.

	$I^3$ in a single grid cell for a surface wind equal to the 99th percentile	DI-SSI contribution in a single grid cell for a surface wind equal to the 99th percentile
Iceland	$2.05 \times 10^{-4}$	0.71
Corsica	$1.24 \times 10^{-3}$	0.67
Theoretical value	–	0.69

The effect of the gaps in the two histograms shown in Figure 1 (top panel) can be shown on grid cell level as well: Figure 1 (bottom panel) depicts the quotient of

the local 99th and 98th percentile (as the division by the 98th percentile is part of the calculation of the SSI) and the average storm frequency per grid cell per extended winter season (i.e. how often on average a windstorm track is detected within a 500 km radius of a particular grid cell). Klawns and Ulbrich (2003) calculated the same quotients for station data of wind speeds in various locations in Germany. Their conclusion was that the quotient was sufficiently homogeneous for the entire country. This assumption can be supported and confirmed by Figure 1 (bottom). Values above 1.1, however, indicate grid cells which are potentially affected by large SSI values, thus in particular Southern Europe. These areas coincide with regions of little storminess over the winter period (less than 8–10 windstorm events per year).



**Table 2.** Integral SSI and DI-SSI values for some prominent European windstorms. The rank of severity for the respective index is denoted in parenthesis. Note that storms which occurred outside of the main storm tracks feature relatively large SSI values (e.g. Klaus, Martin, Xynthia, Torsten) compared to the ones within the main storm track (Daria or Jeanette). This applies especially for the SSI/DI-SSI values per time step. The largest discrepancy in terms of rank of the integral values is observed for Martin and for Vivian/Klaus for time step based values.

Storm	Date	Integral SSI value	Integral DI-SSI value	SSI per timestep	DI-SSI per timestep	References
Daria	23–26 January 1990	26.69 (7)	1940.20 (4)	2.05 (8)	149.25 (5)	Heming (1990)
Vivian	25–28 February 1990	58.52 (2)	4126.34 (1)	3.90 (4)	275.10 (1)	McCallum and Norris (1990)
Anatol	2–4 December 1999	23.57 (8)	1565.67 (6)	1.81 (9)	120.44 (8)	Ulbrich et al. (2001)
Martin	26–28 December 1999	43.81 (4)	1435.09 (8)	5.48 (2)	179.39 (3)	Ulbrich et al. (2001)
Torsten	10–13 November 2001	15.94 (9)	789.95 (9)	2.66 (6)	131.66 (7)	Tripoli et al. (2005)
Jeanette	25–31 October 2002	32.53 (6)	1576.27 (5)	2.32 (7)	112.60 (9)	Parton et al. (2009)
Kyrrill	15–24 January 2007	53.03 (3)	2439.57 (2)	4.08 (3)	187.66 (2)	Fink et al. (2009)
Klaus	23–28 January 2009	74.30 (1)	2117.52 (3)	5.72 (1)	162.89 (4)	Liberato et al. (2011)
Xynthia	26 February to 7 March 2010	37.92 (5)	1459.10 (7)	3.45 (5)	132.65 (6)	Lumbroso and Vinet (2011)

Regarding a potential loss in these areas, large integral SSI values are possibly intentional. Due to a lack of severe large scale storms, the infrastructure might not be as adapted to severe wind speeds as it is in regions within the main storm track. This study, however, aims at creating a metric for the extremeness of a storm using an alternative approach. In order to compare the severity of storms independently from their geographical occurrence, a metric is developed that accounts for the wind speed distribution at a given grid cell. Particularly, the shape of the upper tail of the local wind speed distribution is considered. Due to that feature and its resemblance to the original SSI, the index is named Distribution-Independent SSI (DI-SSI). The DI-SSI can be seen as a side development to the original SSI as it represents a complementary method to assess the severity of storms. The DI-SSI is particularly useful when comparing storms occurring in and outside of the main storm corridor. The two indices are correlated with the North Atlantic Oscillation (NAO), as it is currently recognized to be the most prominent driver of the inter annual variability of European storminess (e.g. Donat et al., 2010; Pinto et al., 2009 or Ulbrich and Christoph, 1999). Due to its parametric nature it is expected that the DI-SSI gives a more coherent and distinct link for areas outside of the classic storm track as it is a smoother function compared to the highly variable nonparametric SSI signal.

## 2. Data and methods

### 2.1. Data and event identification

The wind speed data used for this work are taken from the ERA Interim reanalysis (Dee et al., 2011) which is managed by the European Centre for Medium Range Forecasts (ECMWF). The spectral resolution of ERA Interim is T255 which corresponds to a grid cell size of  $0.7^\circ \times 0.7^\circ$  at the equator. An objective wind-speed-based tracking algorithm (Leckebusch et al., 2008; Kruschke, 2015) was applied to the 6-hourly 10-m wind field of the extended boreal winter

period (October to March) in order to extract wind-storm trajectories. ERA Interim has been frequently used in other ETC studies (e.g., Hodges et al., 2011). The NAO time series is obtained as the first principal component of a rotated EOF analysis of monthly (October to March) mean 700 hPa geopotential height anomalies for the North Atlantic domain ( $70^\circ\text{W}$ – $40^\circ\text{E}$ ,  $30^\circ$ – $80^\circ\text{N}$ ) as done by Hunter et al. (2016).

### 2.2. The DI-SSI

The derivation of the DI-SSI is based on the idea that excesses over a sufficiently large threshold can be well approximated by a generalized Pareto distribution (GPD). The approach of modelling excesses is one of the main concepts within extreme value theory (see e.g. Coles, 2001). Modelling excesses of geophysical data with a GPD has been proposed in various other studies in connection with extreme precipitation [e.g. Vrac and Naveau, 2007 or Cooley et al., 2007], wind speeds (Kunz et al., 2010) and also SSI values (Donat et al., 2011 or Held et al., 2013).

The concept of the DI-SSI is to understand the numerator of the SSI equation (Equation (1)) as the exceedance of a threshold (i.e. the 98th percentile). In contrast to the common method of determining a threshold for the GPD, the threshold is fixed at the 98th percentile for every grid cell. The goodness of fit test provides satisfying results for this threshold (see below). A new variable is introduced to which the GPD is applied:  $v^*$  is defined as the random variable of the excess wind speeds over the local 98th percentile  $v_{98,k}$  at grid cell  $k$  and time  $t$ :

$$v^* = v_{k,t} - v_{98,k} | v_{k,t} > v_{98,k} \quad (3)$$

Estimating parameters of the GPD for  $v^*$  (using the *ismev* library in R; Heffernan and Stephenson, 2015) results in a pair of shape ( $\xi$ ) and scale parameters ( $\sigma$ ) for every grid cell. To get an idea of how well the GPD performs in describing  $v^*$  in the mid-latitudes, a Kolmogorov-Smirnov test (ks-test) is used to assess the goodness of fit of the GPD distribution at every single grid point. Most grid cells over the North Atlantic

and Europe do not show distances larger than the critical value  $D$  of the ks-test at the 5% significance level. Between 30° and 70°N, only 6% (2578 grid cells out of 43520) of all grid cells fail the test. A potential spatial dependence of neighbouring grid cells is neglected as each grid cell is considered as an individual contributor to the DI-SSI, although spatial dependence would potentially increase the amount of rejected cells. Being aware of the weaknesses of the ks-test when distributional parameters are estimated from the sample and the multiple-testing setting, we still consider this test as evidence that a GPD represents a sufficiently good model of  $v^*$  in our region of interest. To avoid the problem with estimated distributional parameters, one could simulate the distribution of the test-statistic under the Null for every grid point. However, we consider this as too costly for the scope of this study here.

Analogous to the equiprobability transformation to yield the Standardized Precipitation Index (SPI; Lloyd-Hughes and Saunders (2002)), the GPD fitted cumulative probability distribution of  $v^*$  is transformed into a standard exponential distribution as the GPD is closely related to the exponential family (rate  $\lambda = 1$ ; cf. Lloyd-Hughes and Saunders (2002), their Figure 1). Equation (4a) defines the transformed value  $x$  by equating the GPD for  $v^*$  with the exponential probability distribution for  $x$ . The resulting Equation (4b) gives the contribution to the DI-SSI ( $x$  in Equation (4b)) of a single grid cell where  $\xi$  represents the shape and  $\sigma$  the scale parameter of the GPD distribution.

$$1 - \left(1 + \frac{\xi v^*}{\sigma}\right)^{-\frac{1}{\xi}} = 1 - e^{-x} \quad (4a)$$

$$\frac{1}{\xi} \ln \left(1 + \frac{\xi v^*}{\sigma}\right) = x \quad (4b)$$

The definition of the (integral) DI-SSI in turn is the result of the summation over the entire footprint of a respective storm, equivalent to the definition of the SSI (cf. Equations (1) and (5)).

$$\text{DI-SSI}_{T,K} = \sum_t \sum_k \left[ \frac{1}{\xi} \ln \left(1 + \frac{\xi v^*}{\sigma}\right) \cdot A_k \right] \quad (5)$$

### 3. DI-SSI in practice and in comparison the SSI

The 99th percentile of the original wind speed distribution  $V_k$  at grid cell  $k$  is equal to the 50th percentile of  $v^*$  (as only wind speeds above the 98th percentile are considered). By definition of the standard exponential distribution, its 50th percentile (median) is equal to  $\ln 2 = 0.69$ . Thus, a wind speed  $v_k$  equal to the 99th percentile results in a DI-SSI contribution of 0.69. In the same way, the 99.9th percentile of  $V_k$  is equal to a contribution of  $-\ln 0.05 = 3.00$  (cf. Equation (4b)). By using these values, the DI-SSI becomes more readily interpretable: The average integral DI-SSI value per

time step of storm Kyrill is 187.66 (cf. Table 2). This value divided by 3.0 (or  $\ln 2$ , respectively) represents an equivalent number of  $1 \times 1$  degree reference grid cells that feature the 99.9th (99th) percentile. Thus for Kyrill this corresponds to around 63 (270) ‘virtual’ grid cells per time step in which the local 99.9th (99th) percentile was observed. In order to compare the SSI contributions to its DI-SSI equivalents, both were calculated for the grid cells described in Section 1.2. As opposed to the SSI contribution for that particular grid cell, which differs by a factor of almost 20, the DI-SSI contribution is almost equal for the two wind speeds (see Table 1).

Table 2 presents integral values of the SSI and DI-SSI for some of the most prominent European windstorms. As expected storms that occurred on the edges of the classical storm track yield comparatively large SSI values. One of the most striking examples is represented by windstorm Klaus (Liberato *et al.*, 2011) whose SSI value is almost three times as large as the respective value for windstorm Daria (Heming, 1990), whereas their DI-SSI values are almost of the same magnitude. Similar conclusions can be drawn from the storms Klaus and Kyrill (Fink *et al.*, 2009): The DI-SSI is similar for both events; however the SSI is about 1.5 times larger for Klaus. Thus, judging from the SSI it appears that storm Klaus was far more intense than both Daria and Kyrill. The different assessment of severity for storms in different climatic background conditions is even more striking when comparing average SSI/DI-SSI values per time step. Klaus and Martin (Ulbrich *et al.*, 2001) which follow similar tracks across Southern and Central Europe exhibit the largest SSI values per time step whereas the largest DI-SSI per time step can be identified for Vivian and Kyrill. Daria, Klaus and Vivian show the largest difference in rank if assessed by the average value per time step. The largest DI-SSI is associated with the storm Vivian (McCallum and Norris, 1990) which ranks second with regard to the SSI ranking. The large magnitude of the DI-SSI can potentially be explained by very extreme winds observed over the Atlantic Ocean (cf. Figure S1, Supporting information). As shown for storm Klaus in Section 3.1, the DI-SSI contributions over the sea are considerably larger than for the SSI. Thus, a storm with extreme surface winds over the sea is subject to high DI-SSI values as the DI-SSI is purely based on the singularity of wind speeds without any potential impact consideration. The biggest discrepancy between the respective rankings for the integral values of the storms is observed for storm Martin (4th compared with 8th) which is in line with the arguments for storm Klaus. An application of both indices is shown in Figure 2 (left panel) where the correlation of the annual storm intensity (annual sum of all SSI/DI-SSI contributions within a 500 km radius around a grid cell) and the annual storm occurrence per grid cell is presented. Hunter *et al.* (2016) showed a similar figure (their Figure 4(a)) using the vorticity as a severity metric. The coherent area of significant values over

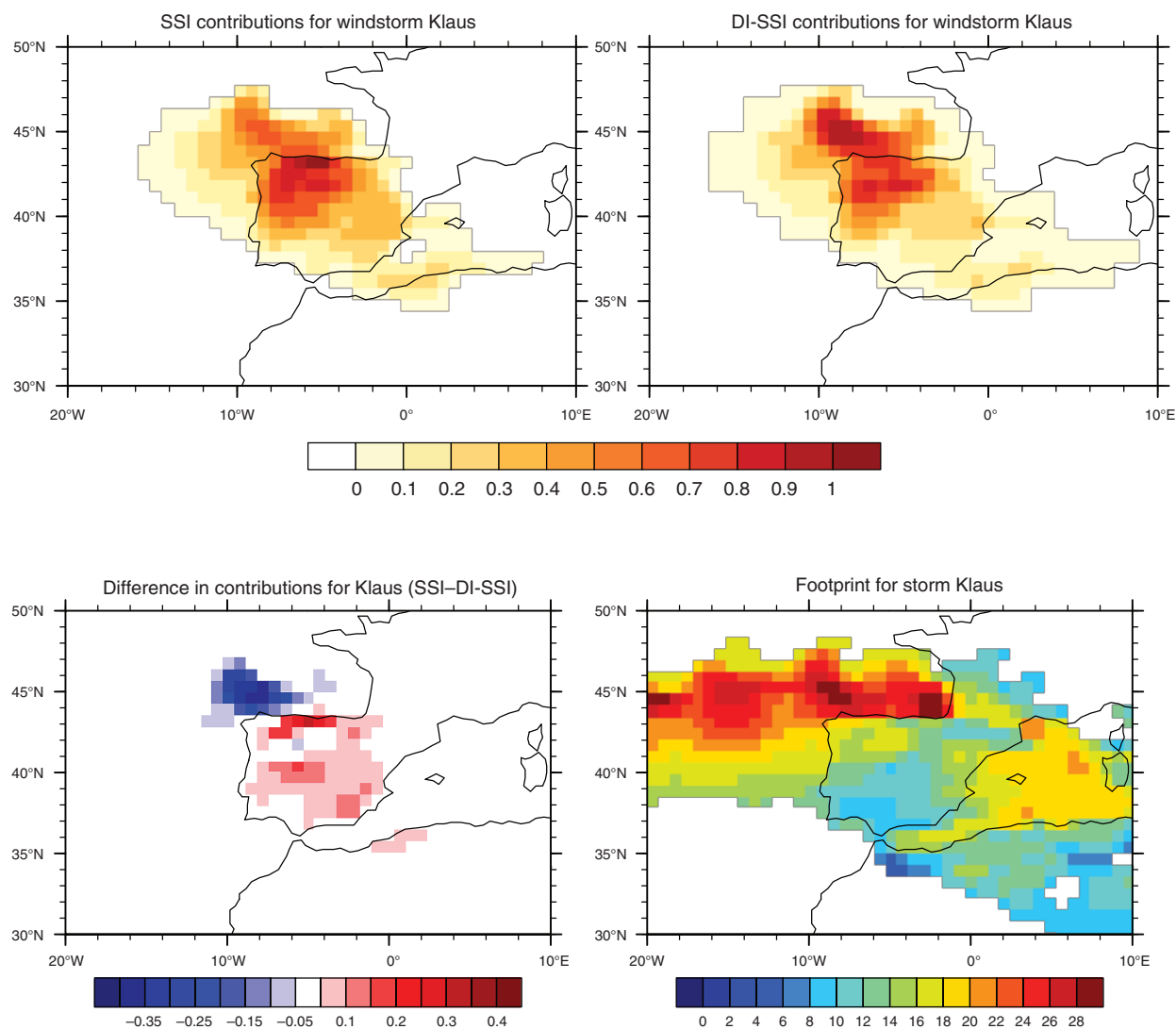


**Figure 3.** Footprint of storm Klaus on 24 January 2009 with SSI contributions shown on the top left, the DI-SSI contributions on the top right and the differences between the both values on the bottom left. The footprint of maximum wind speeds ( $\text{m s}^{-1}$ ) for the entire storm is shown in the bottom right panel. Both SSI and DI-SSI were standardized for comparison reasons. Positive values indicate grid cells with larger SSI contributions value; negative values indicate larger DI-SSI contributions. There is a distinct separation represented by the coast line of the northern and western coast of the Iberian Peninsula.

Scandinavia is smaller compared with their results. The overall pattern looks fairly similar though, with most of Scandinavia showing positive correlations, implying that seasons with more storms also feature more intense storms.

Especially for the DI-SSI (middle-left panel), there is a large area of significant correlation between occurrence and intensity southwest of the British Isles that is not visible in their figure. This indicates the enhanced capability of the DI-SSI to characterize intense and unusual wind speeds not only over land but also over the sea compared with using vorticity as a severity metric. This is in line with the large DI-SSI value for windstorm Vivian for the DI-SSI is capable of quantifying extreme surface winds regardless of their occurrence. This is also supported by the difference between the two correlations shown in the bottom-left panel of Figure 2 as most areas over the Central Atlantic are positive, thus denoting larger DI-SSI correlations.

### 3.1. SSI and DI-SSI compared for a European storm example

Figure 3 serves as an example of how the previously discussed differences between the SSI and the DI-SSI arise: The figure shows a snapshot of the footprint of storm Klaus (Liberato *et al.*, 2011) and the footprint of the entire storm in the bottom right panel. The overall footprint of the storm looks exactly the same by definition as the local 98th percentile is used as a detection criterion in the storm tracking algorithm. The geographical intensity distribution however is different for the two indices (both indices are standardized for comparison). Whereas the SSI has its largest contributions over land on the northern coast of the Iberian Peninsula, the DI-SSI has in fact its largest contributions over the sea just north of the northern coast of Spain. This area coincides with the area of the most extreme wind speeds. This difference becomes more

obvious when looking at the differences of the contributions of both indices. The coast line of the Iberian Peninsula represents an almost perfect segregation between negative and positive differences. This is according to the expectation regarding the features of the SSI and DI-SSI. The SSI can be used well to assess the potential damage to infrastructure, however judging from this figure it would seem that the wind speeds over the Atlantic do not have the same exceedance probability as they have over land. The DI-SSI draws a different picture: Albeit still showing large values over land, the more extreme values are apparent over the ocean indicating that the wind speeds in that area were even more exceptional with regard to their climatological wind speed distribution. This supports the arguments regarding the large DI-SSI for the storm Vivian in Section 3.

### 3.2. Intensity indices in connection with the NAO

A more quantitative comparison is supplied in the right panel of Figure 2. These two figures show the correlation coefficients between the annual winter NAO time series and the annual intensity time series per grid cell for the SSI and DI-SSI, respectively. Grid cells with a correlation coefficient significantly different from zero at the 5% level are stippled. This correlation does not necessarily prove any physical evidence; however, it indicates that the correlation was unlikely if the null hypothesis was true. Considering this fact, both maps show a significant link between the NAO and the intensity of European windstorms for most of Europe. However, overall there are more significant grid cells for the correlation using the DI-SSI compared with the SSI. This applies especially to large parts of southwest France, parts of Northern Africa and some areas in northeast Europe, thus regions which are affected less frequently by large scale windstorms. The largest difference in correlation is observed south of Greenland and around Iceland. According to the bottom panel of Figure 1, these areas are also on the edge of the storm track. This is another indication showing that the DI-SSI is a suitable metric to quantify extreme wind speeds outside the main storm track. The correlation pattern within the main storm track (central North Atlantic) is almost equal for both indices. This supports the expectation that they behave fairly similar given the amount of storms per grid cell is sufficiently large. Thus, the DI-SSI is a useful metric to represent the extremeness of wind speeds both in areas with little annual storm activity and also in areas with increased storminess.

## 4. Summary and discussion

This study introduces the DI-SSI: It serves as a quantification of exceptional surface wind speeds, especially for those high wind speeds occurring outside of the main storm tracks. Due to strongly diverse wind climatologies in different regions, the actual wind speed is an

improper metric for the assessment of extremeness. A widely used index, especially in the impact community is the SSI developed by Leckebusch *et al.* (2008). The SSI is a metric that relates extreme winds to their potential damage on housing or infrastructure, whereas the newly introduced DI-SSI assesses the severity of exceptional wind speeds based on their occurrence probability: The shape of the tail of the local wind climatology is taken into account and used as input regarding the objective severity of an event. Thus, the severity of storms occurring within the main storm track can be compared more accurately to those rarer events, e.g. in the Mediterranean area. SSI/DI-SSI values are presented for nine prominent European winter storms. These values reveal the difference between the two indices. The largest SSI values arise for storms occurring on the edges of the storm track (Klaus, Martin), whereas the DI-SSI ranks storm Vivian and Kyrill as the most severe events.

In connection with the NAO index, the DI-SSI time series shows a more coherent area of significant correlation over Southwest Europe and also the Baltic Sea area compared with the SSI. This proves the capability of the DI-SSI to assess the severity of extreme winds both inside and outside of the main storm track. A larger area of correlation is also apparent for the correlation between frequency and intensity. The overall pattern of correlation for both indices is in agreement with Hunter *et al.* (2016). The results imply that especially within the main storm track in the North Atlantic and for most parts of Scandinavia, seasons with many storms also tend to feature more intense storms. This is in accordance with Vitolo *et al.* (2009) who found that serially clustered seasons are likely to spawn more intense storms. Technically, the SSI is easier to compute than the DI-SSI for it only requires wind speed data on grid cell level and no fitting of a statistical model. The DI-SSI requires more processing of the data, however it is a useful additional tool to assess the severity of storms/extreme winds regardless of their geographic occurrence.

### Acknowledgements

M.A. Walz has been supported by a National Environmental Research Council (NERC) CENTA PhD scholarship kindly funded by Research Councils UK (RCUK). Fragments of this manuscript were prepared as part of a MSc Thesis at Freie Universität Berlin. H. W. Rust received support by the Freie Universität Berlin within the Excellence Initiative of the German Research Foundation. G.C. Leckebusch is supported for his research by the European Union (EU) FP7-MC-CIG-322208 grant. The authors thank the ECMWF for providing ERA Interim reanalysis data. The authors would also like to thank Ben Youngman and an anonymous reviewer for many helpful comments.

### Supporting information

The following supporting information is available:



**Figure S1.** Footprint of maximum wind speed for storm Vivian and Kyrill. The very extreme wind speeds over the Central Atlantic Ocean for Vivian are responsible for the very large DI-SSI value compared to all the other storms which are compared in Table 2. This is due to the fact that the DI-SSI shows the same magnitude for wind speeds of the same extremeness.

## References

- Coles SG. 2001. *An Introduction to Statistical Modeling of Extreme Values*, (Vol. 208). Springer: London.
- Cooley D, Nychka D, Naveau P. 2007. Bayesian spatial modeling of extreme precipitation return levels. *Journal of the American Statistical Association* **102**(479): 824–840.
- Dee D, Uppala S, Simmons A, Berrisford P, Poli P, Kobayashi S, Andrae U, Balmaseda M, Balsamo G, Bauer P. 2011. The ERA-Interim reanalysis: configuration and performance of the data assimilation system. *Quarterly Journal of the Royal Meteorological Society* **137**(656): 553–597.
- Donat MG, Leckebusch GC, Pinto JG, Ulbrich U. 2010. Examination of wind storms over Central Europe with respect to circulation weather types and NAO phases. *International Journal of Climatology* **30**(9): 1289–1300.
- Donat MG, Pardowitz T, Leckebusch GC, Ulbrich U, Burghoff O. 2011. High-resolution refinement of a storm loss model and estimation of return periods of loss-intensive storms over Germany. *Natural Hazards and Earth System Sciences* **11**(10): 2821–2833.
- Fink AH, Brücher T, Ernert V, Krüger A, Pinto JG. 2009. The European storm Kyrill in January 2007: synoptic evolution, meteorological impacts and some considerations with respect to climate change. *Natural Hazards and Earth System Sciences* **9**(2): 405–423.
- Heffernan J, Stephenson A. 2015. Ismev: R package version 1.40, viewed.
- Held H, Gerstengarbe F-W, Pardowitz T, Pinto J, Ulbrich U, Born K, Donat M, Karremann M, Leckebusch G, Ludwig P, Nissen K, Österle H, Prahl B, Werner P, Befort D, Burghoff O. 2013. Projections of global warming-induced impacts on winter storm losses in the German private household sector. *Climatic Change* **121**(2): 195–207.
- Heming J. 1990. The impact of surface and radiosonde observations from two Atlantic ships on a numerical weather prediction model forecast for the storm of 25 January 1990. *Meteorological Magazine* **119**(1421): 249–259.
- Hodges KI, Lee R, Bengtsson L. 2011. A comparison of extratropical cyclones in recent reanalyses ERA-Interim, NASA MERRA, NCEP CFSR, and JRA-25. *Journal of Climate* **24**(18): 4888–4906.
- Hunter A, Stephenson DB, Economou T, Holland M, Cook I. 2016. New perspectives on the collective risk of extratropical cyclones. *Quarterly Journal of the Royal Meteorological Society* **142**(694): 243–256.
- Klawe M, Ulbrich U. 2003. A model for the estimation of storm losses and the identification of severe winter storms in Germany. *Natural Hazards and Earth System Sciences* **3**(6): 725–732.
- Kruschke T. 2015. Winter wind storms: Identification, verification of decadal predictions, and regionalization. Dissertation, Freie Universität Berlin, Berlin, Germany.
- Kunz M, Mohr S, Rauthe M, Lux R, Kottmeier C. 2010. Assessment of extreme wind speeds from Regional Climate Models – Part 1: estimation of return values and their evaluation. *Natural Hazards and Earth System Sciences* **10**(4): 907–922.
- Leckebusch GC, Renggli D, Ulbrich U. 2008. Development and application of an objective storm severity measure for the Northeast Atlantic region. *Meteorologische Zeitschrift* **17**(5): 575–587.
- Liberato ML, Pinto JG, Trigo IF, Trigo RM. 2011. Klaus – an exceptional winter storm over northern Iberia and southern France. *Weather* **66**(12): 330–334.
- Lloyd-Hughes B, Saunders MA. 2002. A drought climatology for Europe. *International Journal of Climatology* **22**(13): 1571–1592.
- Lumbroso D, Vinet F. 2011. A comparison of the causes, effects and aftermaths of the coastal flooding of England in 1953 and France in 2010. *Natural Hazards and Earth System Sciences* **11**(8): 2321–2333.
- McCallum E, Norris W. 1990. The storms of January and February 1990. *Meteorological Magazine* **119**(1419): 201–210.
- Osinski R, Lorenz P, Kruschke T, Voigt M, Ulbrich U, Leckebusch G, Faust E, Hofherr T, Majewski D. 2016. An approach to build an event set of European windstorms based on ECMWF EPS. *Natural Hazards and Earth System Sciences* **16**(1): 255–268.
- Palutikof J, Skellern A. 1991. Storm Severity over Britain. A Report to Commercial Union General Insurance, Climatic Research Unit, School of Environmental Sciences, University of East Anglia, Norwich (UK).
- Parton G, Vaughan G, Norton E, Browning K, Clark P. 2009. Wind profiler observations of a sting jet. *Quarterly Journal of the Royal Meteorological Society* **135**(640): 663–680.
- Pinto JG, Zacharias S, Fink AH, Leckebusch GC, Ulbrich U. 2009. Factors contributing to the development of extreme North Atlantic cyclones and their relationship with the NAO. *Climate Dynamics* **32**(5): 711–737.
- SwissRe. 2016. Natural Catastrophes and Man-Made Disasters in 2015: Asia suffers substantial losses. Sigma No 1/2016. Order number: 270\_0116\_EN.
- Tripoli G, Medaglia C, Dietrich S, Mugnai A. 2005. The 9–10 November 2001 Algerian flood. *Bulletin of the American Meteorological Society* **86**(9): 1229.
- Ulbrich U, Christoph M. 1999. A shift of the NAO and increasing storm track activity over Europe due to anthropogenic greenhouse gas forcing. *Climate Dynamics* **15**(7): 551–559.
- Ulbrich U, Fink A, Klawe M, Pinto J. 2001. Three extreme storms over Europe in December 1999. *Weather* **56**(3): 70–80.
- Vitolo R, Stephenson DB, Cook IM, Mitchell-Wallace K. 2009. Serial clustering of intense European storms. *Meteorologische Zeitschrift* **18**(4): 411–424.
- Vrac M, Naveau P. 2007. Stochastic downscaling of precipitation: from dry events to heavy rainfalls. *Water Resources Research* **43**(7): W07402.